Conf-821133--1

CONF-821133--1

DE83 003484

NOTICE

PORTIONS OF THIS REPORT ARE ILLEGIBLE. It has been reproduced from the best available copy to permit the broadest possible availability.

STRUCTURE OF CERAMIC SURFACES MODIFIED BY ION-BEAM TECHNIQUES*

C. J. McHargue, H. Naramoto,** C. W. White,
J. M. Williams, B. R. Appleton, P. S. Sklad, and
P. Angelini
Oak Ridge National Laboratory
Oak Ridge, Tennessee 37830

INTRODUCTION

Modification of the near-surface region of materials by use of energetic ion beams has been investigated extensively in recent years. The nature of the process allows one to introduce any element into the near-surface region of solids in a controlled and reproducible manner that is independent of most equilibrium constraints. Since the process is nonequilibrium in nature, compositions and structures unattainable by conventional methods may be produced.

In ion implantation, the dopant or alloying element is the ion beam which after an acceleration of tens to hundreds of kiloelectron volts impinges upon the surface of the target (host material). The energetic ion comes to rest by displacing atoms from their normal lattice sites by atomic collisions; thus producing a large number of point defects. After injection, the implanted ions have an approximate Gaussian distribution which is peaked at a fraction of a micrometer beneath the free surface.

Since ceramic materials are particularly sensitive to surface conditions, we have initiated a program to determine the structure

*Research sponsored by the Division of Materials Sciences, U.S. Department of Energy, under contract W-7405-eng-26 with the Union Carbide Corporation.

**On assignment from Physics Division, JAERI, Tokai-mura, Japan.

MASTER

DISCLAIMER

This report was prepared as an account of work sponsored by an agency of the United States Government. Neither the United States Government nor any agency thereof, nor any of their employees, makes any warranty, express or implied, or assumes any legal liability or responsibility for the accuracy, completeness, or usefulness of any information, apparatus, product, or process disclosed, or represents that its use would not infringe privately owned rights. Reference herein to any specific commercial product, process, or service by trade name, trademark, manufacturer, or otherwise, does not necessarily constitute or imply its endorsement, recommendation, or favoring by the United States Government or any agency thereof. The views and opinions of authors expressed herein do not necessarily state or reflect those of the United States Government or any agency thereof.

By acceptance of this article, the publisher or recipient acknowledges the U.S. Government's right to retain a nonexclusive, royalty-free license in and to any copyright covering the article.

and properties of several classes of ceramics whose near-surface region have been modified by a variety of ion beam methods.

Previous studies of ion implantation into Al_2O_3 have dealt largely with changes in optical properties,[1-3] characterization of the disorder produced by the implantation process,[4-8] or the volume changes produced by implantation of gas atoms.[1,9,10]

The optical absorption band produced in Al_2O_3 by particle irradiation has been ascribed to aluminum vacancies[1] or to anion (oxygen) vacancies.[2] The lattice location experiments of Carnera et al.[6,7] showed implanted lead atoms to occupy octahedral interstitial sites that were significantly displaced along the <0001> axis.

Naguib and Kelly[11] include Al_2O_3 in their list of materials that become amorphous during ion bombardment. This conclusion was based on results from gas-release studies,[12] Rutherford backscattering (RBS),[4] and reflection electron diffraction patterns.[13] A transmission electron microscopy (TEM) study by Rechtin, however, indicated the structure of Al_2O_3 implanted with helium, oxygen, neon, or carbon to remain crystalline with a defect structure largely characteristic of that produced by electron or neutron irradiation.[14]

Investigations of the structure and electrical properties of ion implanted silicon carbide have been reported.[15-24] The amount of disorder, as measured by RBS, saturates at the value for a random sample for both nitrogen and antimony.[15-20] Once the amount of lattice disorder, as measured by ion scattering/channeling techniques, equals that from a randomly oriented specimen, it is considered that the material has become amorphous, although Raman spectroscopy indicates some characteristic crystalline bonding may remain.[22-23]

Krypton implantation into sputtered TiB_2 films has been reported to cause blistering and increased adherence to the substrate.[25] The latter effect may have been caused by ion beam mixing with the stainless steel substrate.

EXPERIMENTAL PROCEDURE

Single crystals of α-Al_2O_3 were obtained from Union Carbide Corporation (Crystal Products Division) and Crystal Systems, Inc. Crystals from both suppliers were of high purity (>100 ppm total cation impurities) and contained a low dislocation density ($\sim 10^3$ cm^{-2}). Specimens oriented within 2° of (0001) were polished and then annealed for five days in air at 1200°C to remove any

residual mechanical damage. Single crystal [0001] samples of α-SiC were obtained from the Carborundum Company as platelets produced in an Acheson furnace.

The polycrystalline TiB_2 was prepared at ORNL from Starck powder which initially contained ∿1% oxygen as the major impurity. Specimens having 98.4% theoretical density were prepared by vacuum hot pressing at 2050°C under 25 MPa uniaxially applied pressure for 4 h. The grain size was in the range of 75 to 100 μm.

An Extrion 200 kV ion implantation accelerator was used to implant 10^{16} to 10^{17} ions·cm^{-2} of ^{52}Cr (particle energy of 280 or 300 keV), ^{48}Ti (150 keV), and ^{90}Zr (150 keV) into Al_2O_3 at an orientation 7° off axis at nominally room temperature. The concentration of implanted ions corresponded to 1.6 to 10.0% of the cations initially present in the crystal. A part of each specimen was shielded from the ion beam by a metal mask to preserve a virgin region as a reference state. The same equipment was used for the SiC implants. Fluences from 2.7×10^{13} to 8.1×10^{16} ions·cm^{-2} of ^{14}N (62 keV) and 2.9×10^{14} to 3.1×10^{16} ions·cm^{-2} of ^{52}Cr (280 keV) were used. The ^{58}Ni implantations into TiB_2 were carried out on the ORNL 5 MV Van de Graaff facility to give a fluence of 1×10^{17} ions·cm^{-2} (corresponding to a peak concentration of 16.7% cations).

Annealing of the Al_2O_3 was conducted in air for periods of 1 h at temperatures between 600 and 1600°C. The TiB_2 was annealed for 2 h in vacuum at 1450°C.

The single crystal specimens were examined using Rutherford backscattering-ion channeling techniques (RBS-C) with 2.0 MeV $^4He^+$ to determine the depth profile of the implanted species, the depth distribution of damage in the host lattice, and the lattice location of the impurity. Transmission electron microscopy specimens, prepared by ion milling, with the plane of observation both parallel and perpendicular to the implantation beam were employed to determine the structural characteristics of the implanted zone. Surface profilometry* gave data on the volume changes introduced by implantation. Raman spectroscopy gave important information regarding the structure of implanted SiC.

DISCUSSION OF RESULTS

Figure 1 shows typical spectra of 2.0 MeV He^+ scattered from an Al_2O_3 single crystal in both a random and channeling orientation. The random reference spectrum was obtained from the as-implanted (1×10^{17} ^{52}Cr·cm^{-2}, 300 keV) crystal by continuously rotating it to average over many crystallographic orientations. Ion channeling

*DEKTAK, Sloan Technology Corporation, Santa Barbara, CA.

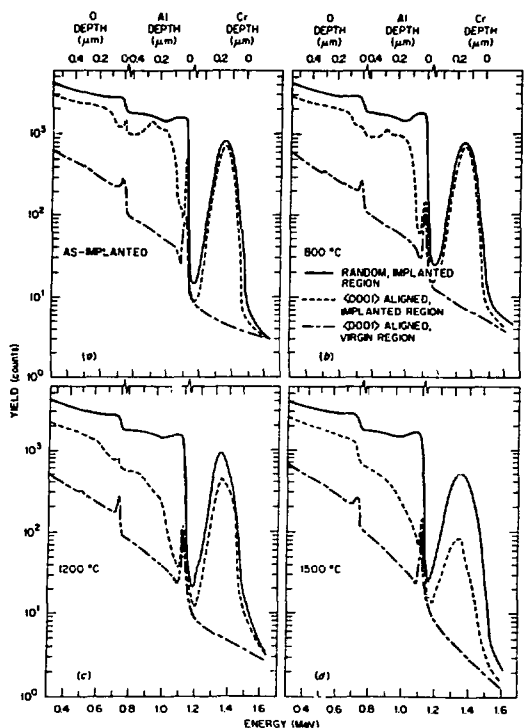

Fig. 1. Rutherford backscattering-channeling spectra for 2 MeV He^+ from chromium-implanted Al_2O_3 (300 keV, 1×10^{17} cm^{-2}). (a) As-implanted; annealed at (b) 800°C, (c) 1200°C, and (d) 1500°C.

spectra were obtained with the ion beam incident parallel to <0001> of both implanted and virgin Al_2O_3. The random spectrum is characteristic of the scattering yield from a completely disordered Al_2O_3 sample while the <0001> virgin shows the yield reduction caused by the channeling effect in a perfect Al_2O_3 crystal. Utilizing the mass specificity of the Rutherford scattering process and the known energy loss of He^+, the scattered energies of Fig. 1 have been converted to separate depth scales for Cr, Al, and O in Al_2O_3. The spectra in Fig. 1(a) show that the Al_2O_3 crystal lattice has been heavily damaged by the chromium implantation. Note, however, that the channeled yield from the as-implanted sample never reaches the random value, indicating that the near-surface region was not totally disordered. This is true for all the implanted species studied (Cr, Zr, Ti, Ni, Fe, and Ge).

The relative damage to the aluminum and oxygen sublattices was seen to saturate for implantation doses from 5×10^{15} to 1×10^{17} $Cr \cdot cm^{-2}$. Utilizing the ion-channeling geometry to detect

preferential lattice locations of the implanted species,[28] it was found that chromium atoms showed only a slight bias toward substitutionality in the samples implanted with 1 x 10^{17} $Cr\cdot cm^{-2}$.

An α-Al_2O_3 specimen implanted to 2 x 10^{16} $Cr\cdot cm^{-2}$ was examined at 1 MV accelerating potential in the ORNL Hitachi 1000 microscope. The diffraction pattern showed the implanted region to be crystalline despite the large amount of damage. The TEM images contained a high density of "black spots," suggestive of point defect clusters. Attempts to determine the character of these clusters were unsuccessful due to large residual stresses in the thinned foils.

Figures 2(a) and 3(a) contain the RBS-C spectra for Al_2O_3 implanted with 2 x 10^{16} $Zr\cdot cm^{-2}$ and 3 x 10^{16} $Ti\cdot cm^{-2}$, respectively. The description given above for Fig. 1(a) applies to these curves also. There is substantial damage to both sublattices but the material is not amorphous. Both figures indicate random (interstitial and substitutional) solid solutions for concentrations of zirconium and titanium which exceed the equilibrium solid solubility.

An analysis of Figs. 1(b–d), 2 (b–d), and 3(b–c) reveals the effects of thermal annealing on the lattice damage and the redistribution and lattice sites of the implanted species in α-Al_2O_3. Damage recovery began selectively in the aluminum sublattice at a temperature of ∿800°C for the chromium-implanted material [Fig. 1(b)]. There was little or no change at this temperature in either the damage distribution in the oxygen sublattice or the degree of chromium substitutionality. At 1000°C, recovery of the oxygen sublattice began but again there was no significant change in the chromium substitutionality [Fig. 1(c)]. After a 1200°C anneal, there was significant incorporation of chromium into substitutional (aluminum) lattice sites and ∿80% of the damage to the aluminum sublattice had recovered.

The effects of higher temperature annealing treatments are summarized in Fig. 4. Figure 4(a) shows that the concentration of chromium as a function of depth is the same after annealing to 1500°C as in the implanted condition. However, ion channeling showed that annealing to 1500°C caused 98% of the chromium to acquire substitutional sites.[28] Detailed angular scans about <0001>, <1$\bar{2}$10>, {10$\bar{1}$0}, {0001}, {1$\bar{2}$10}, and {10$\bar{1}$0} showed conclusively that >98% of the chromium was substitutional in the aluminum sublattice after the 1500°C anneal.[28] However, after the 1300°C anneal some chromium and oxygen remained in interstitial positions. Measurements utilizing EPR showed that the substitutional chromium was largely, if not totally, in the Cr^{+3} state.[28] Further annealing to 1600°C [Fig. 4(a)] resulted in significant redistribution in depth of the chromium but with no loss in substitutionality.

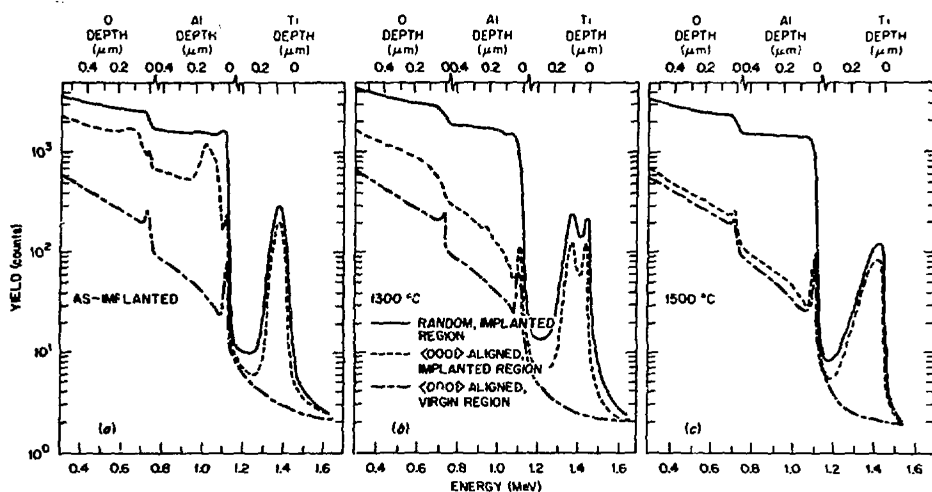

Fig. 2. RBS-C spectra from Ti-implanted Al_2O_3 (150 keV, 3 x 10^{16} cm^{-2}). (a) As-implanted, (b) 1300°C anneal, and (c) 1500°C anneal.

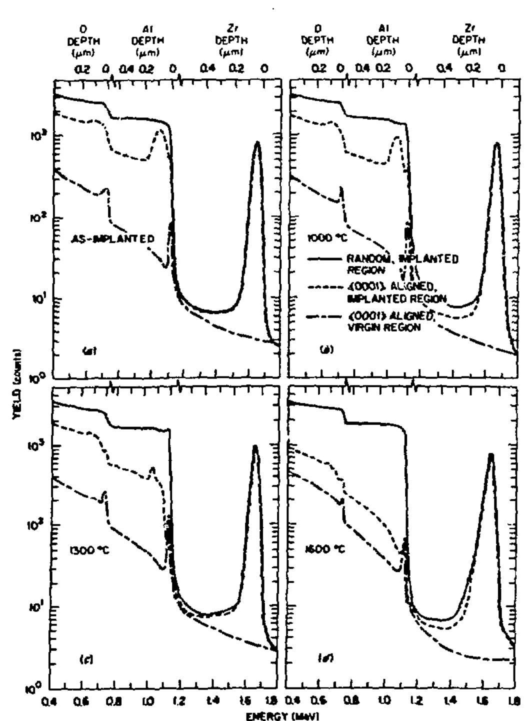

Fig. 3. RBS-C spectra from Zr-implanted Al_2O_3 (150 keV, 2 x 10^{16} cm^{-2}). (a) As-implanted; annealed at (b) 1000°C, (c) 1300°C, and (d) 1600°C.

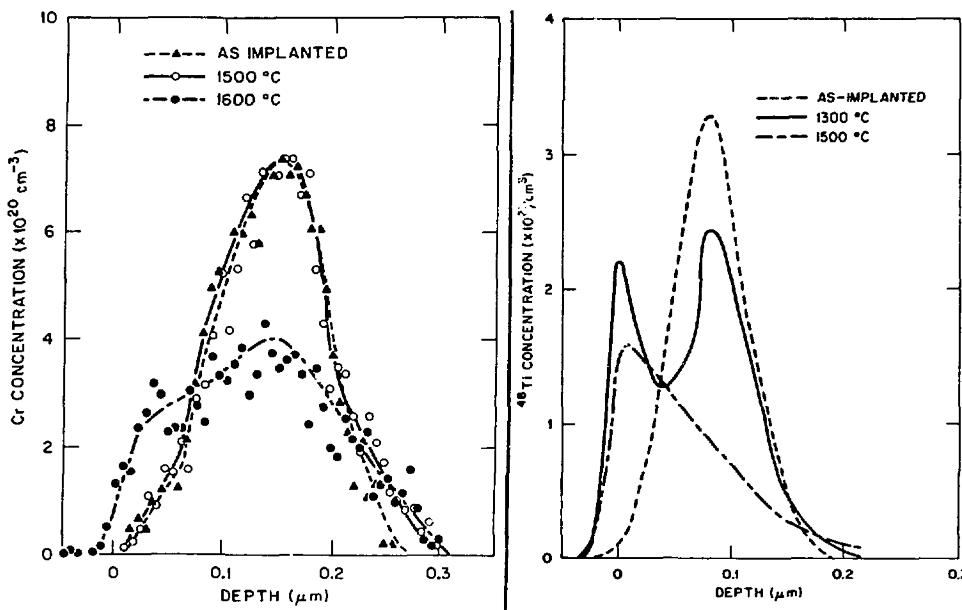

Fig. 4. Concentration profiles for (a) Cr (300 keV, 1×10^{16} cm^{-2}), (b) Ti (150 keV, 3×10^{16} cm^{-2}) in Al_2O_3 for as-implanted condition and after annealing.

From a detailed examination of the chromium spectra in Fig. 1(a–d), one can deduce that during annealing below 1200°C damage recovery in the aluminum sublattice competed with chromium incorporation. Chromium incorporation at higher annealing temperatures appears to be accompanied by oxygen indiffusion from the surface.

The annealing behavior of the titanium-implanted Al_2O_3 differed significantly from the Cr-Al_2O_3 specimens. Again, recovery in the aluminum sublattice began at ∿800°C and in the oxygen sublattice at ∿1000°C. After the 1500°C anneal, recovery was essentially complete [Fig. 2(c)]. However, the titanium spectrum of Fig. 2(b) (1300°C anneal) exhibited a double peak, showing that some of the titanium had diffused toward the surface. This specimen had about 60% of the titanium in substitutional sites. Optical microscopy and TEM revealed that two titanium-rich phases had precipitated. The TEM photograph of Fig. 5 shows one precipitate to be acicular and oriented parallel to <10$\bar{1}$0>. From the work of Philips et al.[29] one would expect this phase to be TiO_2. There is a second precipitate which is much smaller (10–90 nm) and disk shaped. Diffraction patterns have not yet been identified but EDS shows these particles to contain a large amount of titanium. A third feature of these photographs is a large number of small (∿15 nm) voids or bubbles.

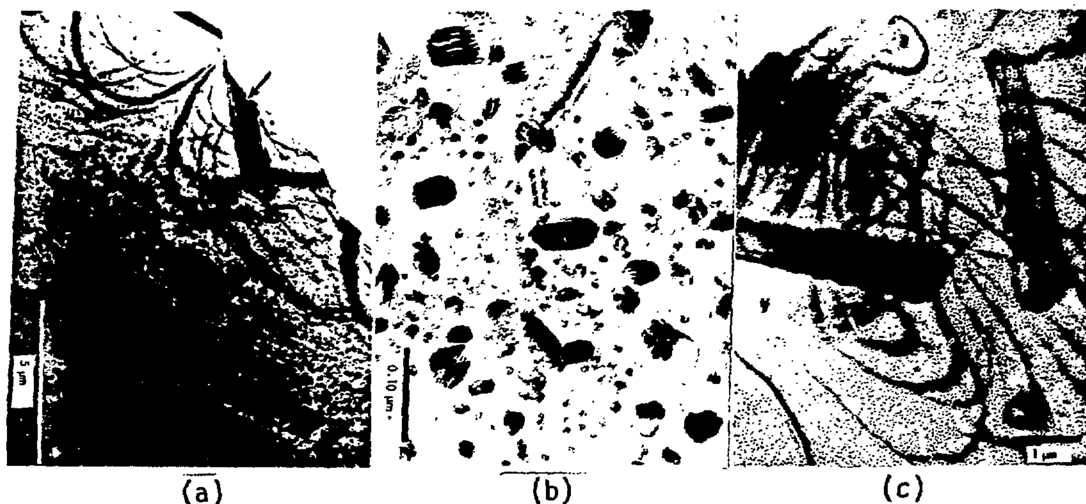

Fig. 5. TEM of back-thinned specimen Al_2O_3 implanted with 3 x 10^{16} Ti-cm^{-2} and annealed at 1100°C. (a) Large precipitates, (b) fine precipitates, and (c) voids or gas bubbles.

Further annealing to 1500°C enhanced the damage recovery [Fig. 2(c)] and caused the bulk of the titanium to diffuse toward the surface [Fig. 4(b)]. Specimens implanted and examined along the <1$\bar{2}$10> direction did not exhibit this redistribution; hence, it can be concluded that diffusion along the *c*-axis is much faster than along the *a*-axis. The diffusion occurs in a temperature range where the titanium was largely distributed randomly suggesting, perhaps, an interstitial diffusion mechanism.

In contrast to the above results, annealing to 1500°C caused no change in the RBS-C spectra for zirconium and the onset of damage recovery was shifted to higher temperatures [Fig. 3(b–d)]. Damage recovery in the oxygen sublattice started at ∿1300°C and, although recovery in the aluminum sublattice began at ∿800°C, large amounts of disorder remained in both sublattices even after annealing at 1600°C. The zirconium exhibited no substitutionality, and no redistribution occurred from the implanted zone. Such observations would be consistent with the precipitation of the zirconium at an early stage of annealing.

The TEM photograph of Fig. 6 confirms that a zirconium-rich second phase was present after the 1300°C anneal. The precipitates were 5 to 20 nm in size but their structure or composition has not been determined. The channeling results suggest that the second phase formed at the lowest annealing temperature (600°C). The precipitates in the 1500°C annealed specimen had about the same size distribution as at 1300°C indicating that, whereas the phase nucleates very early, its growth is slow.

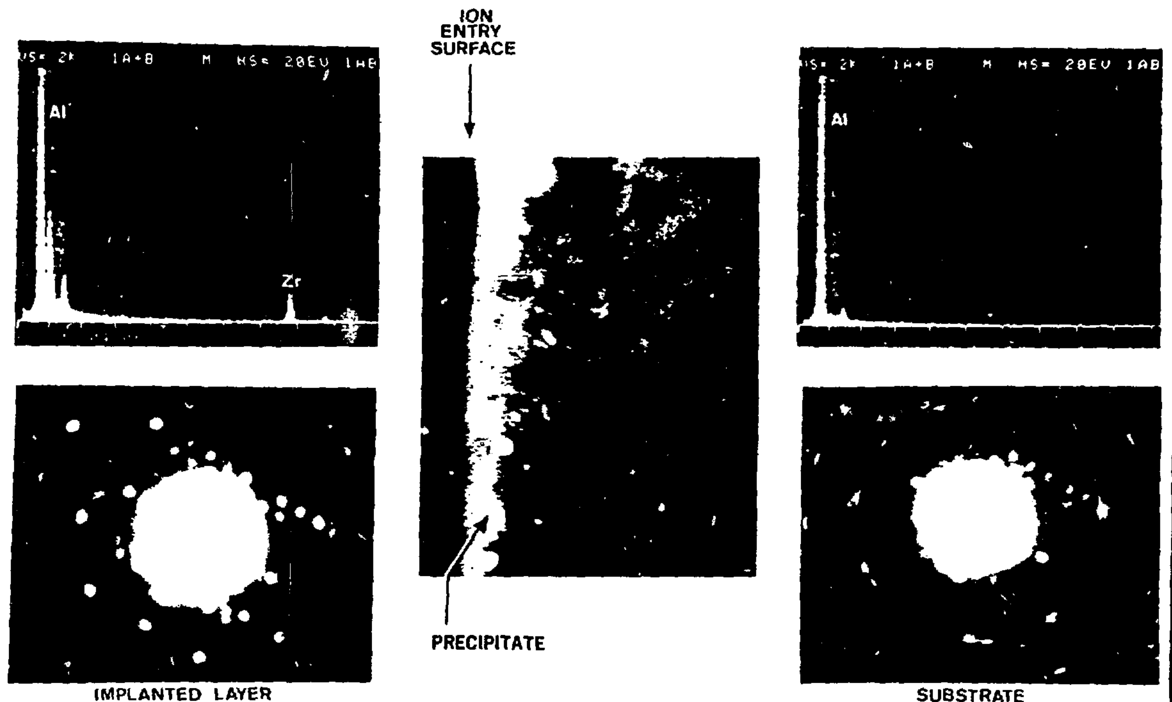

Fig. 6. Dark field TEM, electron diffraction patterns and EDS analysis of Zr-implanted Al_2O_3 (2×10^{16} cm^{-2}) after annealing at 1300°C.

Ion-channeling analyses of single crystals of SiC implanted with nitrogen or chromium to various fluences showed that the channeled ion-scattering yields reached the random yield when implanted doses corresponded to about 0.2 displacements per atom.[30] Figure 7 contrasts a [0001] channeling spectrum for a crystal implanted with 2.9×10^{14} $Cr \cdot cm^{-2}$ with the [0001] channeling and rotating random reference spectra taken from an unimplanted (virgin) SiC single crystal. For this fluence, the damage induced by the implanted chromium ions has "randomized" the crystal in a region 0.02 to 0.2 nm from the surface. This is the region where the damage energy was a maximum and brackets the range where it exceeded the critical value of 0.2 dpa. At higher fluences, the random region spreads in both directions. The dose dependence of randomization for each ion is given in ref. 30.

It is generally assumed that an overlapping of the aligned spectrum with the random spectrum indicates an amorphous structure. In order to determine if this was the case for the present study, TEM and Raman spectroscopy were used to examine the Cr-implanted SiC specimens. The TEM micrograph showed halos in the diffraction patterns characteristic of amorphous material to a depth of 0.25 μm and crystalline patterns at greater depths.[27] The range of 280 keV chromium ions in SiC is ~0.25 μm. The Raman spectra for the virgin

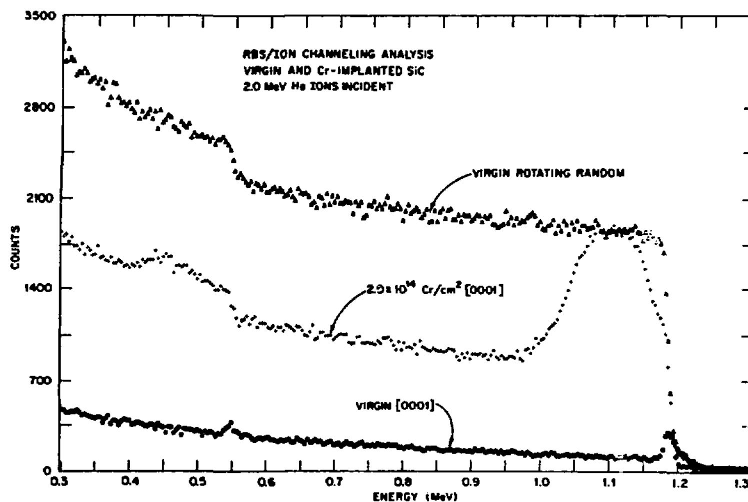

Fig. 7. RBS spectra from α-SiC implanted with Cr.

region contained peaks at 768.13, 784.51, 796.15, and 959.95 cm^{-1} which are characteristic of crystalline SiC.[23,24] After implantation to 2 x 10^{15} $Cr \cdot cm^{-2}$ these crystalline modes were absent, confirming the ion channeling and TEM observations on the amorphous nature of the implanted region.

Because only polycrystalline TiB_2 was available, the techniques used to characterize its implanted structure were limited. Figure 8 shows the TEM results for TiB_2 implanted with 1 x 10^{17} $Ni \cdot cm^{-2}$ (1 MeV). The diffraction patterns show that the surface region remained crystalline. The TEM micrograph shows damage extending to ∿0.8 μm from the surface which consists of a near-surface region with a "coarse damage" structure and an interior region of "fine damage." Studies to determine the nature of the damage are in progress.

The existence of damage to ∿0.8 μm was surprising since the penetration depth of 1 MeV nickel ions in TiB_2 is about 0.4 μm. However, our calculations show that a boron ion which receives the maximum energy transfer in a primary knock-on with a 1-MeV Ni ion would have this range. The titanium recoil range would be about the same as the nickel range. Thus, because of the large difference in the masses of Ti and B, two damage regions are formed: the one nearer the surface due primarily to the displacement of the heavier ions and the other due to the displacement of the lighter ions.

SUMMARY

A wide variety of structures are produced by ion implantation in ceramics. Random (substitutional and interstitial site

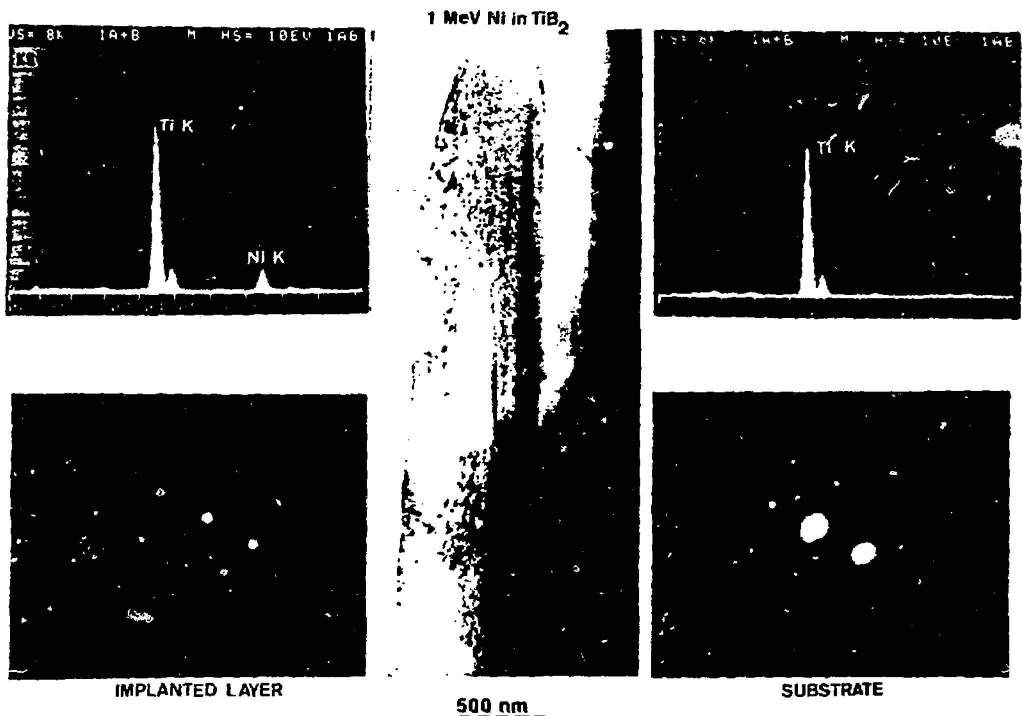

Fig. 8. TEM, electron diffraction and EDS results for TiB_2 implanted with 1×10^{17} $Ni \cdot cm^{-2}$ (1 MeV).

occupancy) solid solutions with concentrations of solute that exceed the solubility limit can be produced in Al_2O_3. The changes that occur during annealing are complex and sometimes unpredictable.

Silicon carbide becomes amorphous in a manner analogous to Si for ion fluences that produce more than 0.2 dpa damage. Light (N) and heavy (Cr) ions produce similar results if the fluence is scaled to damage energy deposited.

Because of mass differences in the ions, two damage regions are developed in TiB_2. The structure remains crystalline to very high damage levels.

These structural alterations cause changes in the surface mechanical properties. Since virtually any chemical species can be implanted, one can independently control structural damage and chemical effects. When coupled with selective annealing, this technique has the potential for producing a wide range of surface structures and properties.

REFERENCES

1. G. W. Arnold, G. B. Krefft, and C. B. Norris, Appl. Phys. Lett. 25:540–42 (1974).
2. B. D. Evans, H. D. Hendricks, F. D. Bazzarre, and J. M. Bunch, in: "Ion Implantation in Semiconductors-1976," F. C. Chernow, J. A. Borders, and D. K. Brice, eds., Plenum Press, New York, (1976), pp. 265–74.
3. T. F. Luera, J. A. Borders, and G. W. Arnold, ibid, pp. 285–94.
4. H. M. Naguib, J. F. Singleton, W. A. Grant, and G. Carter, J. Mater. Sci. 8:1633–40 (1973).
5. A. V. Drigo, S. Lo Russo, P. Mazzoldi, P. D. Goude, and N.E.W. Hartley, Radiat. Eff. 33:161–71 (1977).
6. A. Carnera, A. Drigo, and P. Mazzoldi, Radiat. Eff. 49:29–32 (1980).
7. A. Carnera, G. Della Mea, A. V. Drigo, S. Lo Russo. P. Mazzoldi. and N.E.W. Hartley, Radiat. Eff. 35:201 8 (1978).
8. A. Turos, H. Matzke, and P. Rabette, Phys. Stat. Sol.(a) 64: 565–75 (1981).
9. G. B. Krefft, W. Beezhold, and E. P. EerNisse, IEEE Trans. Nucl. Sci. NS-22:2247–49 (1975).
10. G. Krefft and E. EerNisse, J. Appl. Phys. 49:2725–30 (1978).
11. H. M. Naguib and R. Kelly, Radiat. Eff. 25:1-12 (1975).
12. C. Jech and R. Kelly, J. Phys. Chem. Sol. 30:465–74 (1969); 31:41–8 (1970).
13. H. Matzke and J. L. Whitton, Canad. J. Phys. 44:995-1010 (1966).
14. M. D. Rechtin, Radiat. Eff. 42:129–44 (1979).
15. O. J. Marsh and H. L. Dunlap, in: "Ion Implantation," F. Eisen and L. T. Chadderton, eds., Gordon and Breach, New York (1970), pp. 285–95.
16. R. Hart, H. Dunlap, and O. Marsh, Radiat. Eff. 9:261–66 (1971).
17. O. J. Marsh, in: "Silicon Carbide-1973," R. C. Marshall, J. W. Faust, Jr., and C. E. Ryan, eds., University of South Carolina Press (1973), pp. 471–85.
18. A. B. Campbell, J. B. Mitchell, J. Shewchun, D. Thompson, and J. A. Davies, ibid, pp. 486–92.
19. W. J. Choyke, L. Patrick, and P. J. Dean, Phys. Rev. B 10: 2554–65 (1974).
20. A. B. Campbell, J. Shewchun, D. A. Thompson, J. A. Davies, and J. B. Mitchell, in: "Ion Implantation in Semiconductors," S. Namba, ed., Plenum Press, New York (1975), pp. 291–98.
21. D. A. Thompson, M. C. Chan, and A. B. Campbell, Canad. J. Phys. 54:626–32 (1976).
22. R. B. Wright, R. Varma, and D. M. Gruen, J. Nucl. Mater. 63: 415–21 (1976).
23. R. B. Wright and D. M. Gruen, Radiat. Eff. 33:133–40 (1977).
24. V. V. Makarov, T. Tuomi, and K. Naukkarinen, Appl. Phys. Lett. 35:922–24 (1979).

25. K. Padmanabhan and G. Sorensen, Thin Solid Films 81:13-19 (1981).
26. C. J. McHargue, H. Naramoto, B. R. Appleton, C. W. White, and J. M. Williams, in: "Metastable Materials by Ion Implantation," S. T. Picraux and W. J. Choyke, North Holland, New York (1982), pp. 147–53.
27. C. J. McHargue and J. M. Williams, ibid, pp. 303–9.
28. H. Naramoto, C. W. White, J M. Williams, C. J. McHargue, O. W. Holland, M. M. Abraham, and B. R. Appleton, submitted to Journal of Applied Physics.
29. D. S. Philips, A. H. Heuer, and T. E. Mitchell, Phil. Mag. A 42:385-432 (1980).
30. J. M. Williams, C. J. McHargue, and B. R. Appleton, in: "Proceedings of Ion Beam Modification of Materials-1982," to be published in Journal of Nuclear Instruments and Methods.